

Biochemical Circuit Theory for Analysis of Large-Scale Metabolic Networks

Daniel A. Beard¹, Shou-dan Liang², and Hong Qian³,

August 11, 2001

Abstract

Predicting behavior of large-scale biochemical metabolic networks represents one of the greatest challenges of bioinformatics and computational biology. Approaches, such as flux balance analysis (FBA), that account for the known stoichiometry of the reaction network while avoiding implementation of detailed reaction kinetics are perhaps the most promising tools for the analysis of large complex networks. As a step towards building a complete theory of biochemical circuit analysis, we introduce energy balance analysis (EBA), which compliments the FBA approach by introducing fundamental constraints based on the first and second laws of thermodynamics. Fluxes obtained with EBA are thermodynamically feasible and provide valuable insight into the activation and suppression of biochemical pathways.

Conservation principles impose constraints on the fluxes and chemical potentials associated with biochemical network reactions that are analogous to Kirchoff's current and voltage laws for electrical networks (1). Flux balance analysis (2-13) invokes mass conservation, but does not

¹ Department of Bioengineering, University of Washington, Seattle, WA 98195

² NASA Ames Research Center, Moffett Field, CA 94035

³ Departments of Applied Mathematics and Bioengineering, University of Washington, Seattle, WA 98195

consider the chemical potential of non-equilibrium steady state chemical fluxes. The thermodynamic analysis presented here—energy balance analysis (EBA)—provides additional constraints on the system that are analogous to the voltage loop law. In addition to predicting network fluxes that are thermodynamically feasible, EBA facilitates a detailed analysis of regulation of metabolic networks that is not available from FBA alone.

The central flux balance conservation statement is given by the equation:

$$Sf = 0, \quad (1)$$

where $f \in \mathbb{R}^n$ is the vector of n fluxes occurring in the network, $S \in \mathbb{R}^{m \times n}$ is the stoichiometric matrix, and m is the number of reactants in the system. The matrix S stores the stoichiometric coefficients associated with each flux in the network. In the above formulation both internal fluxes and boundary fluxes, which transport material into or out of the system, are included in S . Typically, a number of inequalities are introduced to constrain the boundary fluxes depending upon the external media (7-10, 12, 13):

$$\alpha_i \leq f_i \leq \beta_i. \quad (2)$$

As implemented by Palsson and colleagues (2, 7-13), biological networks are assumed to optimize a certain biologically meaningful objective function, which is a linear combination of the fluxes:

$$Z = \sum_{i=1}^n c_i f_i = c^T f. \quad (3)$$

For example, in the analysis of *E. coli* central metabolism the objective is constructed from the production of biosynthetic precursors required to generate biomass (8, 10). Another example uses maximization of ATP production to simulate mitochondrial energy metabolism (11).

Regardless of the application, optimization of a linear objective function (Eq. 3), together with the equality constraints (Eq. 1) and the inequality constraints (Eq. 2), represents a linear optimization problem, which can be solved with linear programming (14).

The power of FBA is illustrated by the *tour de force* assembly of the complete stoichiometry of the known reactions in *E. coli* central metabolism provided by Edwards and Palsson (8, 10). Edwards and Palsson show that the flux balance simulation of the organism-scale metabolic network predicts the metabolic capabilities of *E. coli* (8, 10). Under various external constraints (e.g. aerobic vs. anaerobic growth) FBA can distinguish between genes essential and not essential for growth in 68 of 79 cases studied (8). This predictive capability of FBA is striking considering the tremendously complex problems that can be modeled using little or no free parameters.

Lacking from FBA is the explicit consideration of the energy balance and thermodynamics of the network reactions. Since biochemical networks are comprised of multiple-species reactions, energy balance loop equations cannot be obtained from topological loops in the network, as is done in electrical circuit analysis (1). However, we will show that the energy balance equations are obtained from an analysis of the network stoichiometry.

If we combine redundant fluxes and remove the columns from S that correspond to boundary fluxes, the remaining matrix, denoted S' , represents the complete set of possible internal chemical transformations. Using the singular value decomposition (14), S' can be decomposed as:

$$S' = A\Lambda B^T, \quad (4)$$

where Λ has the following form:

$$\Lambda = \begin{bmatrix} \lambda_1 & \cdots & 0 & 0 & \cdots & 0 \\ \vdots & \ddots & \vdots & \vdots & & \vdots \\ 0 & \cdots & \lambda_m & 0 & \cdots & 0 \end{bmatrix}. \quad (5)$$

The first m columns of Λ form a diagonal matrix where the diagonal entries are the singular values λ_i . The entries of the remaining columns are all equal to zero. If n_c is the number of columns of S' and r is the rank of S' , then columns $r+1$ through n_c of the matrix B provide the $(n_c - r)$ -dimensional null space of S' . We introduce the matrix K , which stores the null space vectors of S' :

$$K = \begin{bmatrix} B_{1,r+1} & \cdots & B_{m,r+1} \\ \vdots & & \vdots \\ B_{1,n_c} & \cdots & B_{m,n_c} \end{bmatrix}, \quad (6)$$

and we denote the i^{th} row of K as \hat{k}_i . Summing the n_c chemical reactions, each scaled by the corresponding entry of \hat{k}_i , results in a perfectly balanced reaction equation (with same reactants in equal proportion on either side of the equation). An example of this analysis for a simple five-metabolite network with four reactants is illustrated in Fig. 1.

To study network thermodynamics, we consider the vector $\Delta\mu$ that lists the n_c chemical potential differences associated with the reaction fluxes. Since each \hat{k}_i provides weights for exactly balancing the chemical reaction equations (see Fig. 1), solutions to the equation

$$K \Delta\mu = 0 \quad (7)$$

balance the global free energy of the network. Eq. 7 is a statement of conservation of energy, and hence follows from the first law of thermodynamics (15). The second law of thermodynamics takes the form of an inequality constraint for each flux,

$$f_i \cdot \Delta\mu_i < 0, \quad (8)$$

which ensures that each reaction dissipates energy. Note that the first law imposes an equality while the second law imposes an inequality, as expected. Eqs. 7 and 8 represent thermodynamic constraints that should be considered in addition to the flux balance constraints. Eq. 8 provides a link that couples mass balance and energy balance, and constrains the feasible flux space more strictly than Eqs. 1 and 2 alone.

We have obtained the stoichiometric matrix provided by Edwards and Palsson (10), used to represent the flux balances in the *E. coli* central metabolism. The web-posted supplementary information (10) provides detailed descriptions of the reaction network, which contains 953 fluxes (735 internal; 218 boundary) acting on 536 metabolites. Using the MATLAB (The Mathworks Inc., Natick, MA) optimization package we reproduced the linear programming analysis presented in Ref. 10, and optimized the production of biomass with glucose and oxygen uptake constrained to be less than or equal to 10 and 15 mmol g-DW⁻¹ h⁻¹, respectively. The resulting flux produces a growth rate of 0.81 h⁻¹ on glucose minimal media.

To compute the thermodynamic properties of this large-scale network we first combine redundant fluxes (e.g., the phosphofructokinase A and B reactions are combined into a single column of S'), resulting in $n_r = 617$ internal reactions operating on 536 metabolites. The growth is the optimized under the flux balance constraints (Eqs. 1 and 2) and the constraint that the

energy balance equations (Eqs. 7 and 8) are satisfied. We impose the additional constraint that $\Delta\mu$ must be finite for all nonzero fluxes. The free energy can go to zero only if the flux is zero, implying that a given reaction is in chemical equilibrium. This analysis predicts the same optimal growth rate (0.81 h^{-1} on glucose minimal media) as that reported above for FBA. Yet the FBA prediction does not represent a unique solution to the optimization problem because redundancies in the metabolic network allow the optimal growth rate to occur for an infinite number of possible internal flux distributions. Since the EBA-constrained solution is (at least in this case) able to achieve the same optimal growth rate as that obtained by considering only the FBA constraints, the fluxes obtained by EBA represent one particular optimal solution to the FBA linear programming problem. However, optimal flux distributions obtained by considering flux balance alone are not necessarily thermodynamically feasible. The EBA constraints further restrict the set of feasible fluxes, and provide a more physically realistic flux distribution. Selected fluxes from glycolysis, TCA cycle, and respiration are tabulated in Fig. 2. Fluxes from the wild type on glucose media under aerobic and anaerobic conditions are labeled WT (oxygen) and WT (anaerobic), respectively.

EBA further allows quantitative estimation of the chemical potentials in the system. First, we introduce the *flux resistances*, defined as $r_i = -\Delta\mu_i / f_i$. To avoid the unphysical situation in which $\Delta\mu_i = 0$ for a finite f_i , which is equivalent to setting the flux resistance equal to zero, we assume that there exists a minimum flux resistance, r_{\min} (which is equivalent to saying that there exists an upper limit to the effective reaction rate constants). Thus the second law constraint is modified:

$$\Delta\mu_i \leq -r_{\min} f_i, \quad f_i > 0$$

$$\Delta\mu_i \geq +r_{\min} f_i, \quad f_i < 0. \quad (9)$$

Realistically, each flux may have a different r_{\min} . However for our purposes we find that a single value, $r_{\min} = 400 \text{ kcal mol}^{-2} \text{ g-DW h}$, produces reasonable behavior and can be used to describe the entire network (16). The energy balance constraint can alternatively be written in terms of the chemical potentials (Eq. 7) or the flux resistances:

$$[K] \begin{bmatrix} f_1 & & 0 \\ & \ddots & \\ 0 & & f_{n_c} \end{bmatrix} \begin{bmatrix} r_1 \\ \vdots \\ r_{n_c} \end{bmatrix} = K \cdot \text{diag}(f) \cdot r = 0. \quad (10)$$

With the fluxes fixed using the values obtained from the above analysis, we use quadratic programming to find an optimal $\Delta\mu$ that minimizes the norm of the free energy vector $|\Delta\mu|^2$. In addition to the fluxes, Fig. 2 lists the predicted chemical potentials and the conductances, $c_i = r_i^{-1}$, of each reaction. The choice of $r_{\min} = 400 \text{ kcal mol}^{-2} \text{ g-DW h}$ results in reasonable predictions of chemical potential. For example, $\Delta\mu_i = -9.55 \text{ kcal mol}^{-1}$ for ATP hydrolysis.

The reaction conductance provides a measure of the activation level of the pathway. If $c_i = 0$ then the associated enzyme(s) is not present or is deactivated. Increases in flux or conductance, at a fixed free energy, indicate that a pathway is up regulated, at either the expression level or the post-translational level. By changing the boundary constraints, we can study how the metabolic network responds to changes in substrate. In Fig. 2 we compare the predicted EBA fluxes and free energies for the WT cell grown under aerobic and anaerobic conditions. We identify a pathway as “down regulated” (colored blue) if the flux conductance decreases by a factor of 4 or more, and “up regulated” (colored green) when the conductance increases by more than a factor

of 4. Based on this analysis we identify three enzymes that require activation upon moving from aerobic to anaerobic conditions: fumarate reductase, pyruvate formate lyase, and pyridine nucleotide transhydrogenase. Other pathways show increases or decreases in flux compared to aerobic growth. However these differences can be accounted for by changes in the free energy and thus do not necessarily require regulation.

Following the work of Edwards and Palsson (8, 10) we studied the effects of gene knockouts on the metabolic capabilities of *E. coli*. We found that *zwf*, *pgl*, and *gnd* knockouts result in the same predicted phenotype (Fig. 2), with only two up regulations compared to WT: succinate dehydrogenase and pyridine nucleotide transhydrogenase. Again, a number of predicted fluxes that differ from the WT do not require up regulation of the associated enzymes. The situation is similar for *pyk* and *pgi* knockouts. The *pyk* knockout requires an up regulation of phosphoenolpyruvate carboxylase to maintain growth of almost 99% that predicted for WT. No other significant regulations are predicted. The *pgi* knockout analysis predicts one significant up regulation and three down regulations and a similar growth rate. Thus, we find that *much of the capacity for metabolic control is built in to the wild type expression and activation levels. Few regulatory steps are required when nonessential genes are knocked out; the network is robust and tolerant to errors and deletions (17,18).*

However, the situation is different when essential genes are knocked. The *eno* and *pfk* genes are examples of genes that FBA falsely identifies as nonessential to growth on glucose minimal media (8). The fact that *eno* and *pfk* are essential for growth in vivo (19) may be related to the demands that the knockouts of these genes place on metabolic regulatory mechanisms. These

demands are much heavier than those imposed by nonessential knockouts. Our analysis predicts that maintaining growth with these knockouts requires a greater number of pathway regulations than for the nonessential knockouts. Of the 64 reactions listed in Fig. 2, 15 are predicted to be upregulated and 15 downregulated for the *pfk* knockout. Thus, the predicted phenotype is markedly different from the wild type for nearly half of the reactions associated with glycolysis, TCA cycle, and respiration, while the *pyk* and *pgi* knockouts differ very little from WT.

These predictions are based on one major simplification—that the entire network can be characterized by a single r_{\min} , or equivalently a maximum pathway conductance. More realistically, constraints could be placed on each pathway based on a priori knowledge of the biochemistry. One promising aspect of EBA is that it is possible to incorporate as much, or as little, as is known about the individual reactions. For example, if we know that the ratio $[ATP]/[ADP]$ in the cell is greater than the equilibrium ratio (20), then we know that the free energy of ATP hydrolysis satisfies the inequality:

$$\Delta\mu_{ATP \rightarrow ADP} \leq \Delta\mu^o_{ATP \rightarrow ADP} = -7.3 \text{ kcal mol}^{-1}. \quad (11)$$

In general, consider the reaction $A \rightarrow B$. If the ratio $[A]/[B]$ is greater than 1, then the free energy of that reaction is constrained $\Delta\mu_i < \Delta\mu_i^o$. Alternatively, if the concentration ratio is less than 1, then $\Delta\mu_i > \Delta\mu_i^o$. If the reactant concentrations are known, then the constraint becomes an equality: $\Delta\mu_i = -k_B T \ln(K_{eq}[A]/[B])$, where k_B is Boltzmann's constant, T is the absolute temperature, and K_{eq} is the equilibrium constant of the reaction.

Together, flux balance and energy balance provide basic laws for the analysis of biochemical networks. These laws, akin to the basic principles of circuit theory for electrical networks, make the analysis and design of large-scale biochemical systems practical. The engineering approach to analysis and design of such complex systems is the identification of modular components that are separable within the system (21). Flux balance and energy balance circuit theory provides a basis for understanding how these modules function and interact.

References and Notes

1. N. Balabanian, T. A. Bickart, *Linear Network Theory: Analysis, Properties, Design, and Synthesis* (Matrix, Beaverton, OR, 1981).
2. A. Varma, B. O. Palsson, *Biotechnology* 12, 994, (1994).
3. H. P. J. Bonarius, et al., *Biotechnol. Bioeng.* 50, 299, (1996).
4. J. Pramanik, J. D. Keasling, *Biotechnol. Bioeng.* 56, 398, (1997).
5. H. P. J. Bonarius, G. Schmid, J. Tramper, *Trends Biotechnol.* 15, 308, (1997).
6. S. Schuster, T. Dandekar, D. A. Fell, *Trends Biotechnol.* 17, 53, (1999).
7. C. H. Schilling, S. Schuster, B. O. Palsson, and R. Heinrich, *Biotechnol. Prog.* 15, 296, (1999).
8. J. S. Edwards, B. O. Palsson, *Proc. Natl. Acad. Sci. USA* 97, 5528, (2000).
9. J. S. Edwards, B. O. Palsson, *Biotechnol. Prog.* 16, 927 (2000).
10. J. S. Edwards, B. O. Palsson, *BMC Bioinformatics* 1, 1 (2000). Supplementary data available at http://gcrp.ucsd.edu/supplementary_data/BP2000/main.htm.

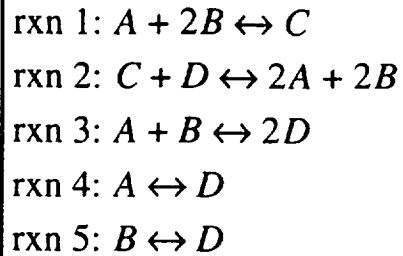
11. R. Ramakrishna, J. S. Edwards, A. McCulloch, B. O. Palsson, *Am. J. Physiol.* 280, R695, (2001).
12. C. H. Schilling, J. S. Edwards, D. Letscher, B. O. Palsson, *Biotechnol. Bioeng.* 71, 286, (2001).
13. J. S. Edwards, R. U. Ibarra, B. O. Palsson, *Nat. Biotechnol.* 19, 125, (2001).
14. G. Strang, *Introduction to Applied Mathematics* (Wellesley-Cambridge Press, Wellesley, MA, 1986).
15. D. A. McQuarrie *Statistical Thermodynamics* (University Science Books, Mill Valley, CA, 1973).
16. Note that by replacing the constraint of Eq. 9 with Eq. 8 (e.g., setting the minimum flux resistance to zero), several values of $\Delta\mu_i$ approach zero for a number of reactions with nonzero fluxes. For example, the adenylate kinase reaction $\text{GTP} + \text{AMP} \leftrightarrow \text{ADP} + \text{GDP}$ is found to have a flux of about $1.75 \text{ mmol g-DW}^{-1} \text{ h}^{-1}$, but a potential of zero (within numerical tolerance). Such a situation would require tremendously high concentrations of GTP, AMP, ADP, and GDP to proceed in the steady state.
17. H. Jeong et al., *Nature*, 407, 651, (2000).
18. N. Barkai, S. Leibler, *Nature* 387, 913, (1997).
19. D. G. Fraenkel, in *Escherichia Coli and Salmonella Cellular and Molecular Biology*, F. C. Neidhardt et al., Eds. (ASM Press, Washington DC, 1996), vol. 1, ch. 14. [second edition]
20. L. Stryer, *Biochemistry* (W. H. Freeman and Co., New York, 1995). [fourth edition]
21. L. H. Hartwell, J. J. Hopfield, S. Leibler, A. W. Murray, *Nature*, 402, C47, (1999).

22. We thank Dr. J. B. Bassingthwaite for constant insight and support and Dr. J. S. Edwards and Dr. B. O. Palsson for providing the *E. coli* central metabolism stoichiometric matrix and for helpful discussion. The work supported by NIH grants NCRR-1243 and NCRR-12609.

Figure Legends

Figure 1: Illustration of energy balance equations for a network of five reactions. The first step is determination of the stoichiometric matrix from the reactions in the network. For this example, the stoichiometric matrix has rank $r = 3$, resulting in 2 independent null space vectors. The null space vectors provide mutually orthogonal solutions to $S'f = 0$. In addition, the null space vectors are the rows of the matrix K , the energy balance matrix for which $K \Delta G = 0$.

Figure 2: Regulation of reactions in glycolysis, TCA cycle, and respiration. Predicted biochemical fluxes (in $\text{mmol g-DW}^{-1} \text{ h}^{-1}$), chemical potentials (in kcal mol^{-1}), and conductances (in ??) are reported for 64 central metabolic reactions, for wild type (WT) aerobic and anaerobic growth, and for *zwf*, *pgl*, *gnd*, *pyk*, *pgi*, *eno*, and *pfk* knockouts. Predicted growth rate for each case is reported in units of hr^{-1} . Green and blue shading indicate up and down regulation relative to WT, respectively. Yellow indicates that a reversible flux has changed direction. Gray shading indicates that the flux cannot be identified as a site of regulation because, although the conductance has changed moderately (by less than a factor of 10), the magnitudes of the free energy and the flux have both either increased or decreased. "N.P." denotes enzymes that are not present under given conditions. "Eq." refers to reactions that are at equilibrium, for which the conductance cannot be estimated. All simulations are performed for glucose minimal media.

Reaction Network:**Stoichiometric Matrix:**

	rxn 1	rxn 2	rxn 3	rxn 4	rxn 5
A	-1	+2	-1	-1	0
B	-2	+2	-1	0	-1
C	+1	-1	0	0	0
D	0	-1	+2	+1	+1

Null Space Vectors: $\hat{k}_1 = [0.5630, 0.5630, 0.4148, 0.1483, -0.4148]$
 $\hat{k}_2 = [0.2409, 0.2409, -0.4505, 0.6914, 0.4505]$

Stoichiometric Balance Equations:

$$K_{1,1} \cdot (\text{rxn 1}) + K_{1,2} \cdot (\text{rxn 2}) + K_{1,3} \cdot (\text{rxn 3}) + K_{1,4} \cdot (\text{rxn 4}) + K_{1,5} \cdot (\text{rxn 5})$$

$$= 2A + 2B + C + D \rightarrow 2A + 2B + C + D$$

$$K_{2,1} \cdot (\text{rxn 1}) + K_{2,2} \cdot (\text{rxn 2}) + K_{3,3} \cdot (\text{rxn 3}) + K_{4,4} \cdot (\text{rxn 4}) + K_{5,5} \cdot (\text{rxn 5})$$

$$= 2A + 2B + C + D \rightarrow 2A + 2B + C + D$$

Energy Balance Equations:

$$K \Delta\mu = \begin{bmatrix} \hat{k}_1 \\ \hat{k}_2 \end{bmatrix} \begin{bmatrix} \Delta\mu_1 \\ \vdots \\ \Delta\mu_5 \end{bmatrix} = 0$$

Enzyme	Gene(s)	WT (aerobic)			WT (anaerobic)			zwf (or pgi or gnd)			pyk			pgi			eno			pfk		
		flux	ΔH	c	flux	ΔH	c	flux	ΔH	c	flux	ΔH	c	flux	ΔH	c	flux	ΔH	c	flux	ΔH	c
Glucose phosphotransferase	pcrG	10	-4	2.5	10	-4	2.5	10	-4	2.5	10	-4	2.5	10	-4	2.5				1.3418	-0.5367	2.6
Glucokinase	glk	0	-7.0082	0	0	-3.7652	0	0	-8.369	0	0	-4.3242	0	0	-4.1363	0						
PGI (G-6-P / F-6-P)	pgi	2.3309	-1.2083	1.9291	3.0918	-6.4891	0.8978	3.0918	-6.4178	0.8978	1.2058	-1.8777	0.6422				-0.3327	0.8987	0.6175	-3.7913	0.1831	
PGI (BDG-6-P / G-6-P)	pgi	-1.5104	0.8041	2.5	-6.8563	2.7425	2.5	-6.7724	2.709	2.5	-2.3471	0.9388	2.5				0.6734	-0.2894	2.5	7.6906	-3.0762	
PGI (BDG-6-P / F-6-P)	pgi	1.5104	-0.8041	2.5	6.8563	-2.7425	2.5	6.7724	-2.709	2.5	2.3471	-0.9388	2.5				-0.6734	0.2894	2.5	-7.6906	3.0762	
Glucose-1-phosphatase	gsp	0	-1.2708	0	0	-3.6728	0	0	-1.927	0	0	-0.951	0	0	-0.9552	0	0	-6.8044	0			
Phosphofructokinase	pfkB	7.1478	-2.8591	2.5	9.7011	-3.8604	2.5	9.1783	-3.8713	2.5	7.0836	-2.8254	2.5	5.8813	-4.8729	1.2089						
Fructose-1,6-bisphosphatase	fbp	0	-6.6908	0	0	-7.2304	0	0	-8.5518	0	0	-3.4008	0	0	-1.1738	0	0	-3.8448	0	0	0	Eq.
Fructose-1,6-bp aldolase	fba	7.1478	-2.8591	2.5	9.7011	-3.8604	2.5	9.1783	-3.8713	2.5	7.0836	-2.8254	2.5	5.8813	-3.8991	1.5899						
Triphosphate isomerase	tpiA	-7.0684	2.8226	2.5	-9.6689	3.8675	2.5	-9.0898	3.8359	2.5	-8.9735	2.7894	2.5	-6.7915	3.8991	1.5856				0.8982	4	
GAP-dehydrogenase	gapA/CIC2	15.774	-6.3097	2.5	19.217	-7.8869	2.5	17.849	-7.1394	2.5	15.71	-6.2841	2.5	14.532	-5.8127	2.5	14.778	-5.9103	2.5			
Phosphoglycerate kinase	pgkA	15.774	-6.3097	2.5	19.217	-7.8869	2.5	17.849	-7.1394	2.5	15.71	-6.2841	2.5	14.532	-5.8127	2.5	14.778	-5.9103	2.5			
Phosphoglycerate mutase	gpmA/B	14.322	-5.7286	2.5	18.737	-7.4947	2.5	16.442	-6.5787	2.5	14.279	-5.7116	2.5	13.191	-5.2766	2.5	0	0	Eq.			
Enolase	eno	14.322	-5.7286	2.5	18.737	-7.4947	2.5	16.442	-6.5787	2.5	14.279	-5.7116	2.5	13.191	-5.2766	2.5						
Phosphoenolpyr. synthetase	ppsA	0	-4.3797	0	0	-7.7606	0	0	-4.9658	0	0	-2.828	0	0	-2.0828	0						
Pyruvate kinase	pykA,F	1.3145	-0.8041	1.6348	7.5883	-3.0353	2.5	3.5303	-1.4121	2.5												
Pyruvate dehydrogenase	pdhA, aceEF	9.2368	-3.8947	2.5				11.519	-4.8075	2.5	9.2577	-3.7031	2.5	5.0482	-2.0185	2.5	0	0	Eq.			
Glucose-1-P adenyltransferase	glgC	0.1323	-2.8277	0.0468				0.1281	-3.4679	0.0369	0.1303	-1.7252	0.0756	0.13	-1.8663	0.078	0.0947	-2.512	0.0377			
Glycogen synthase	glgA	0.1323	-2.8277	0.0468				0.1281	-3.4679	0.0369	0.1303	-1.7252	0.0756	0.13	-1.8663	0.078	0.0947	-2.512	0.0377			
Glycogen phosphorylase	glgP	0	-2.8277	0	0	-3.5784	0	0	-3.4679	0	0	-1.7252	0	0	-1.8663	0	0	-2.512	0			
Glucose-6-P dehydrogenase	zwf	6.0107	-2.4043	2.5							6.3014	-2.5206	2.5	9.8548	-3.9418	2.5	10.9	-4.3601	2.5	17.903	-7.1612	2.5
6-Phosphogluconolactonase	pgl	6.0107	-2.4043	2.5							6.3014	-2.5206	2.5	9.8548	-3.9418	2.5	10.9	-4.3601	2.5	17.903	-7.1612	2.5
6-Phosphogluconate dehydrog.	gnd	6.0107	-2.4043	2.5							6.3014	-2.5206	2.5	9.8548	-3.9418	2.5	10.9	-4.3601	2.5	17.903	-7.1612	2.5
Ribose-5-P isomerase	rpiA/B	2.6307	-1.0523	2.5							2.7183	-1.0873	2.5	3.9011	-1.5606	2.5	4.0824	-1.833	2.5	6.3737	-2.5495	2.5
Ribose-5-P 3-epimerase	rpe	3.361	-1.3444	2.5	4.2276	-1.7171	2.5				3.5844	-1.4256	2.5	5.9349	-2.3739	2.5	6.8042	-2.7217	2.5	11.517	-4.8089	2.5
Transketolase nm. 1	tdkA/B	1.8536	-0.7414	2.5	-0.0988	0.871	2.5				1.9527	-0.7811	2.5	3.1375	-1.255	2.5	3.526	-1.4104	2.5	5.8708	-2.3482	2.5
Transketolase nm. 2	tdkA/B	1.5074	-0.803	2.5	-0.1748	0.8988	2.5				1.6117	-0.8447	2.5	2.7974	-1.119	2.5	3.2782	-1.3113	2.5	5.6485	-2.2586	2.5
Transaldolase	talB	1.8422	-0.7369	2.5	-0.0988	0.871	2.5				1.9415	-0.7786	2.5	3.1263	-1.2505	2.5	3.5179	-1.4072	2.5	5.8633	-2.3453	2.5
Citrate synthase	glcA	1.42	-3.1849	0.4459	0.9105	-0.1243	2.5	3.2354	-1.2942	2.5	1.2445	-2.5281	0.4923	0.8665	-5.3201	0.1629						
Aconitase	aconA/B	1.42	-3.1849	0.4459	0.9105	-0.1243	2.5	3.2354	-1.2942	2.5	1.2445	-2.5281	0.4923	0.8665	-5.3201	0.1629						
Isocitrate dehydrogenase	icdA	1.42	-0.568	2.5	0.3108	-0.1243	2.5	3.2354	-1.2942	2.5	1.2445	-1.1887	1.0469									
2-Ketoglutarate dehydrogenase	icdA/B, icdA	0.5382	-0.2153	2.5	0	0	Eq.	2.3816	-0.9526	2.5	0.3757	-0.1503	2.5	0	-0.9635	0	0	0	Eq.			
Succinyl-CoA synthetase	sucCD	0.1532	-0.0813	2.5	-0.1285	2.1419	2.5	2.0088	-0.8035	2.5				-0.3763	0.1619	2.5	-0.2767	1.5919	0.1789	-0.2482	0.0897	
Succinate dehydrogenase nm 1	sdhABCD	0.5382	-3.1849	0.169							0.3757	-2.5281	0.1486	0	0	Eq.				0	0	Eq.
Fumarate reductase	frdABCD	0	3.1849	N.P.				0	0.9526	N.P.	0	2.5281	N.P.	0	0	N.P.	0	12.09	N.P.	0	0	N.P.
Fumarase	fumABC	1.4173	-0.5689	2.5	0.2204	-0.0882	2.5	3.2328	-1.2931	2.5	1.2418	-0.4987	2.5	0.8638	-0.3456	2.5	0.8294	-0.2518	2.5			
Malate dehydrogenase	mdh	1.4173	-0.5689	2.5	0.2204	-0.0882	2.5	3.2328	-1.2931	2.5				0.8638	-0.3456	2.5	0.8294	-0.2518	2.5			
D-lactate dehydrog. (Pyr → LAC)	ldhA, ldhA	0	-22.564	0	0	-5.0625	0	0	-26.865	0	0	-16.771	0	0	-16.532	0	0	-36.079	0			
D-lactate dehydrog. (cytochrome)	ldh	0	-22.564	0	0	-5.0625	0	0	-26.865	0	0	-16.771	0	0	-16.532	0	0	-36.079	0			
Acetaldehyde dehydrogenase	adhE	0	0	Eq.	7.8546	-3.1419	2.5	0	0	Eq.	0	0	Eq.	0	0	Eq.	0	0	Eq.	0	0	2.4968
Pyruvate formate lyase	pfABCD	0	-8.7047	0				0	-10.278	0	0	-8.291	0							0	-8.7295	0
Formate hydrogen lyase	ldhA, hycBE	0.0274	-0.011	2.5	8.2435	-3.2974	2.5	0.0134	-0.0064	2.5	0.0138	-0.0054	2.5	1.0597	-0.4239	2.5	4.3095	-1.7238	2.5	0	0	Eq.
Phosphotransacetylase	pta	5.1487	-2.0687	2.5	7.7505	-3.1002	2.5	5.898	-2.2792	2.5	5.3827	-2.1531	2.5	4.7052	-1.8821	2.5	7.5525	-3.021	2.5	-0.2801	3.2248	0.0003
Acetate Kinase	ackA, pntT	5.1487	-2.0687	2.5	7.7505	-3.1002	1.0588	5.898	-2.2792	2.5	5.3827	-2.1531	2.5	4.7052	-1.8821	2.5	7.5525	-3.021	2.5	-0.2801	3.2248	0.0003
Acetyl-CoA synthetase	acs	0	0	Eq.	0	0	Eq.	0	0	Eq.	0	0	Eq.	0	0	2.5	0	0	Eq.	0.0006	-1.8139	0.0003
Phosphoenolpyr. carboxylase	pcrA	0	-3.4038	0	0	0	Eq.	0	-3.4063	0	0	-3.9725	0	0	-2.861	0	0	0	Eq.			
Phosphoenolpyr. carboxylase	ppc	2.3006	-6.1459	0.3743				2.2276	-8.8168	0.2526				2.2608	-3.1856	0.7068						
Malic enzyme (NADP)	malE	0	0	Eq.	0	-1.6771	0	0	0	2.5	1.3106	-0.5242	2.5	0	0	Eq.	0	-6.5011	0	0.0005	-0.0002	2.6
Malic enzyme (NAD)	malA	0	-4.7748	0	0	-3.1235	0	0	-6.1115	0	0	-4.3637	0	0	-5.9357	0	0	-15.106	0			
Isocitrate lyase	aceA	0	-3.3498	0	0	0	Eq.	0	-6.333	0	0	-1.3394	0	0	-3.3935	0	0	-7.0885	0	0	-6.3359	0
Malate synthase A	aceB, glcB	0	-3.3498	0	0	0	Eq.	0	-6.333	0	0	-1.3394	0	0	-3.3935	0	0	-7.0885	0	0	-6.3359	0
Inorganic pyrophosphatase	ppa	2.8681	-1.0864	2.5	0.9391	-0.3757	2.5	2.5814	-1.8196	1.4187	2.6268	-1.0606	2.5	2.6197	-1.0479	2.5						
NADH dehydrogenase II	ndh	0	-45.107	0	0	-10.125	0	0	-63.73	0	0	-33.542	0	0	-33.084	0	0	-72.159	0			
NADH dehydrogenase I	nuoABEF	29.209	-11.683	2.5	0	0	Eq.	27.373	-10.949	2.5	29.375	-11.75	2.5	29.751	-11.9	2.5	29.819	-11.928	2.5	29.832	-11.933	2.5
Formate dehydrogenase N ₂ O	fdhGHI	0	-20.998	0	0	0	Eq.	0	-23.615	0	0	-16.501	0	0	-17.124	0	0	-30.307	0	0	-23.704	0
Glycerol-3-P dehydrogenase	ldhA/HG	0	-24.941	0	0	-5.7857	0	0	-29.921	0	0	-18.708	0	0	-19.5	0	0	-40.382	0			
Cytochrome oxidase bo3	cyoABCD,c	30	-12	2.5	0	0	Eq.	30	-12	2.5	30	-12	2.5	30	-12	2.5	30	-12	2.5	29.995	-11.998	2.5
Cytochrome oxidase bd	cydABCE,a	0	-16.775	0	0	-1.4464	0	0	-18.112	0	0	-15.113	0	0	-15.023	0	0	-20.604	0			
Succinate dehydrogenase nm 2	sdhABCD	0.5456	-25.059	0.0218	-0.0888	0.8947	2.5	2.3816	-0.9526	2.5	0.383	-18.313	0.0209							0.1665	-0.0888	2.5
Thioredoxin reductase	trxB	0.2572	-0.1029	2.5	0.0908	-0.0362	2.5	0.249	-0.0996	2.5	0.2534	-0.1014	2.5	0.2527	-0.1011	2.5	0.1841	-0.0737	2.5	0.1665	-0.0888	2.5
PNT 1	pntAB	0	0	Eq.	0	0	Eq.	0	0	Eq.	1.891	-0.7584	2.5	7.281	-2.9124	2.5	0	0	Eq.	22.204	-8.8818	2.5
PNT 2																						